JACS
JOURNAL OF THE AMERICAN CHEMICAL SOCIETY
Article
pubs.acs.org/JACS

Solubilizing the Most Easily Ionized Molecules and Generating Powerful Reducing Agents

Gina M. Chiarella,[†,§,#] F. Albert Cotton,[†,▽] Jason C. Durivage,[‡,∥,#] Dennis L. Lichtenberger,*[,‡,#] and Carlos A. Murillo*[,†,#]

[†]Department of Chemistry, Texas A&M University, College Station, Texas 77842-3012, United States

[‡]Department of Chemistry and Biochemistry, Center for Gas-Phase Electron Spectroscopy, The University of Arizona, Tucson, Arizona 85721, United States

Supporting Information

ABSTRACT: Two very soluble compounds having W_2(bicyclic guanidinate)$_4$ paddlewheel structures show record low ionization energies (onsets at 3.4 to 3.5 eV) and very negative oxidation potentials in THF (−1.84 to −1.90 V vs Ag/AgCl). DFT computations show the correlation from the gas-phase ionization energies to the solution redox potentials and chemical behavior. These compounds are thermally stable and easy to synthesize in high yields and good purity. They are very reactive and potentially useful stoichiometric reducing agents in nonpolar, nonprotonated solvents.

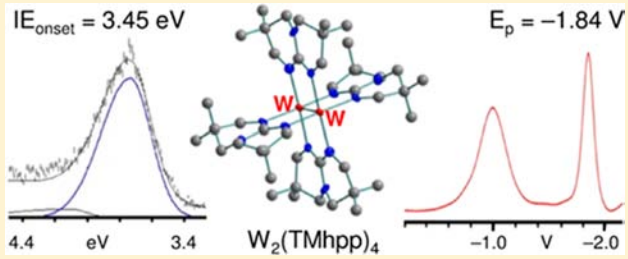

INTRODUCTION

Stable, strong oxidizing and reducing agents have many important chemical and materials applications. Especially needed are strong redox agents to be utilized in nonaqueous, homogeneous systems and for reactions in which stoichiometric control is critical. While studying compounds with metal−metal bonds, we[1] and others[2] have found that bridging bicyclic guanidinate ligands can often stabilize dimetal units in high oxidation states. In some cases, the common M_2^{4+} units become extremely thermodynamically unstable to oxidation, the prime example being W_2(hpp)$_4$ (hpp = the anion of 1,3,4,6,7,8-hexahydro-2*H*-pyrimido[1,2-*a*]pyrimidine; see Chart 1 for ligand representations). With an onset ionization energy of only 3.51 eV, this quadruple bonded W_2(hpp)$_4$ compound has the lowest known ionization energy for any molecule prepared in a synthesis laboratory,[3] being even lower than that of cesium, the most easily ionized stable element.

Chart 1. Bicyclic Guanidinate Anion Ligands in This Work

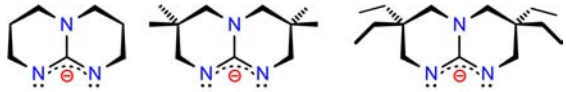

The redox properties of W_2(hpp)$_4$ and its ability to act as a reducing agent were investigated generating mixed results. This compound was found to be very reactive as a reductant,[1c] but a major drawback was the poor solubility in nonreactive organic solvents. To increase the solubility of the ditungsten compounds with bicyclic guanidinates, the ligand has now been modified by adding four nonpolar alkyl substituents to the third and ninth positions of the hpp backbone, making available the anion of 3,3,9,9-tetramethyl-1,5,7-triazabicyclo[4.4.0]dec-4-ene (TMhpp)[4] and the anion of 3,3,9,9-tetramethyl-1,5,7-triazabicyclo[4.4.0]dec-4-ene (TEhpp)[5] ligands (Chart 1). The methyl and ethyl substituents were also expected to lower the ionization energies and induce shifts in the negative direction in the oxidation potentials. The proof of concept was initially reported for dimolybdenum compounds.[6,7]

Here we report the synthesis of two compounds with triple bonded W_2^{6+} cores, namely W_2(TMhpp)$_4$Cl$_2$, **1**, and W_2(TEhpp)$_4$Cl$_2$, **2**, that serve as precursors for the syntheses of W_2(TMhpp)$_4$, **3**, and W_2(TEhpp)$_4$, **4**, respectively. Compounds **1**−**3** have been characterized by X-ray crystallography and either electrochemical properties, photoelectron spectroscopy (PES), or other spectroscopic and spectrometric techniques, and compound **4** has been characterized by ^{1}H NMR and PES. The molecules have excellent properties for strong reducing agents in organic solvents.

RESULTS

Photoelectron Spectroscopy. The photoelectron spectra of the first ionization bands of **3** and **4**, shown in Figure 1 (sample full spectrum in the SI), reveal that the ionization energies vary slightly but nevertheless are visibly lower than the ionization energy of the parent compound W_2(hpp)$_4$. The onset ionization energies for W_2(TMhpp)$_4$, **3**, and W_2(TEhpp)$_4$, **4**, are 3.45 ± 0.03, and 3.40 ± 0.05 eV, respectively (Table 1). These values make **3** and **4** the compounds with the lowest IEs known. For comparison, the IE

Received: August 13, 2013
Published: October 25, 2013

   dx.doi.org/10.1021/ja408291k | J. Am. Chem. Soc. 2013, 135, 17889−17896

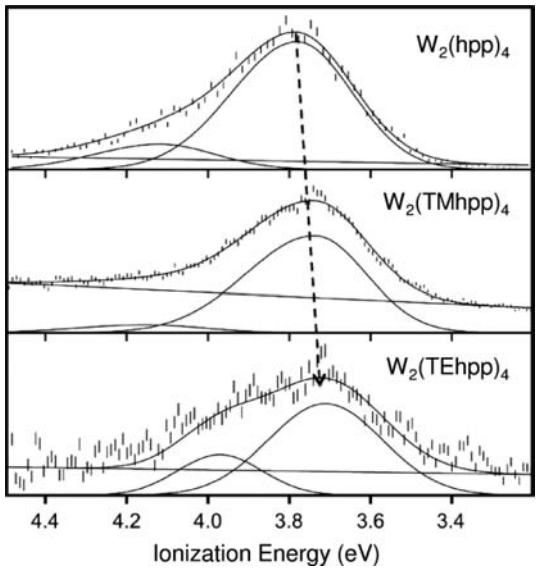

Figure 1. Photoelectron spectra of the low ionization energy regions (δ bond ionizations) of W_2(bicyclic guanidinate)$_4$ complexes. See the Experimental Section and the SI for analysis of the band profiles and energies.

Table 1. Gas-Phase First Ionization Energies (IE in eV)

	$IE_{vertical}$	IE_{onset}
$W_2(hpp)_4$[a]	3.76(2)	3.51(5)
$W_2(TMhpp)_4$	3.74(3)	3.45(3)
$W_2(TEhpp)_4$	3.71(3)	3.40(5)

[a]Ref 3.

for cesium is 3.89 eV.[8] The IE for **3** was measured in the range from 216 to 271 °C over a period of 2.5 h while that for **4** was measured in the range of 317−340 °C for about 1 h. In neither case was there any evidence of decomposition. This indicates that the thermal stability of both compounds in a vacuum is very high. As solids these species are almost indefinitely stable when stored in sealed ampules protected from air and from protonated or halogenated solvents.

Electrochemistry. Electrochemical measurements in THF on **1** and **2** show that each compound has two reversible redox waves at negative potentials. In the differential pulse voltammograms (DPVs), shown in Figure 2,[9] the peaks at −1.84 and −1.90 V vs Ag/AgCl have been assigned to the $W_2^{5+/4+}$

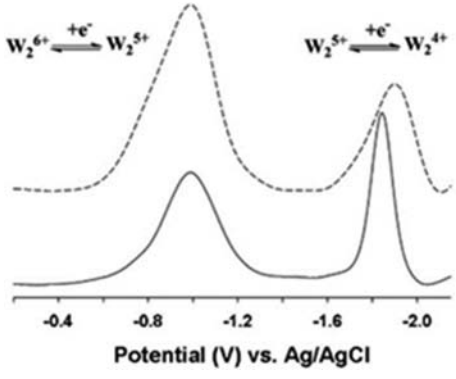

Figure 2. DPVs in THF for $W_2Cl_2(TMhpp)_4$ (solid line) and $W_2Cl_2(TEhpp)_4$ (broken line).

processes for the methyl and ethyl derivatives, respectively, and those at −0.99 and −0.99 V correspond to the $W_2^{6+/5+}$ processes (Table 2). For comparison, for $W_2(hpp)_4$ the

Table 2. First and Second Reduction Potentials in THF (E_p in V vs Ag/AgCl)

	$E_p(1)$	$E_p(2)$
$W_2(hpp)_4Cl_2$[a]	−0.97	−1.81
$W_2(TMhpp)_4Cl_2$	−0.99	−1.84
$W_2(TEhpp)_4Cl_2$	−0.99	−1.90

[a]Ref 10.

reported $E_{1/2}(2)$ is −0.97 V and that for $E_{1/2}(1)$ is −1.81 V.[10] The shifts in the solution oxidation potentials for these molecules are the same as the shifts of the onset gas-phase IEs within experimental uncertainty, indicating that the solvation and thermodynamic effects on the relation between the ionization energies and oxidation potentials are similar for these molecules.[11]

Preparation and Solution Chemistry. The precursors can be easily prepared in good yields using standard Schlenk-type techniques by reaction of commercially available and stable $W(CO)_6$ with the neutral bicyclic guanidinates in refluxing *o*-dichlorobenzene, as shown in Scheme 1. The

Scheme 1. Syntheses

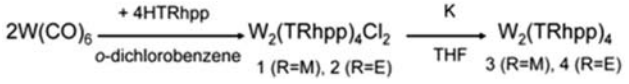

chlorinated solvent is important not only to provide a high reflux temperature but also to serve as the oxidizing agent and be the source of the chlorine atoms in **1** and **2**. Both precursors can be handled in dry air over hours when they are in crystalline form. This makes them convenient sources for weighing and general handling of the compounds previous to further reactions. The compounds can be rapidly reduced to **3** and **4**, respectively, with excess potassium metal in refluxing THF using strict anaerobic conditions. The excess K can be easily removed by filtration, and the THF can be removed for use of **3** and **4** in noncoordinating solvents. Elimination of the THF solvent under vacuum produces essentially quantitative products,[12] as long as crystalline precursors are used, but further purification can easily be accomplished by removing the THF solvent followed by extraction with benzene or toluene. However, the compounds can usually be used in further reactions without the extraction step.

It should be noted that both **3** and **4** are easily oxidized and quickly decompose in air and in the presence of halogenated or protonated solvents. Importantly, these compounds are very soluble in common dry solvents such as THF, toluene, and benzene (Table 3). Some solubility of **3** in hexanes is also observed, while **4** is significantly more soluble in the latter. This is the reason why its structure is not reported (vide infra) since very concentrated solutions yielded only small amounts of poorly diffracting crystals. Solvent retention by **4** also made collection of the gas-phase photoelectron spectrum more difficult and was a factor in the lower signal-to-noise obtained for the spectrum of this molecule.

The solubility properties of **3** and **4** compare very favorably to those of decamethylcobaltocene, a commonly used reducing

dx.doi.org/10.1021/ja408291k | J. Am. Chem. Soc. 2013, 135, 17889−17896

Table 3. General Solubility Properties in Dry Solvents

solvent	$W_2(hpp)_4Cl_2$	$W_2(TMhpp)_4Cl_2$	$W_2(TEhpp)_4Cl_2$
DMSO	soluble	very	very
THF	slightly	soluble	very
benzene	insoluble	soluble	very
toluene	insoluble	soluble	very
hexanes	insoluble	slightly	soluble
	$W_2(hpp)_4$	$W_2(TMhpp)_4$	$W_2(TEhpp)_4$
THF	slightly	very	very
benzene	slightly	very	very
toluene	slightly	very	very
hexanes	insoluble	soluble	very

agent,[13] but it is worth noting that the IEs and electrode potentials of **3** and **4** are significantly more favorable than those of $(Cp^*)_2Co$. The ionization energy of $(Cp^*)_2Co$ at 4.705 eV[13] is more than 1 eV greater than that of **3** and **4**, and the oxidation potential of $(Cp^*)_2Co$ at −1.47 V[12] is ∼0.4 V less negative than that of **3** and **4**.

Structures. The structures of **1**−**3**, provided in Figures 3 and S1 each show a paddlewheel structure with four bicyclic

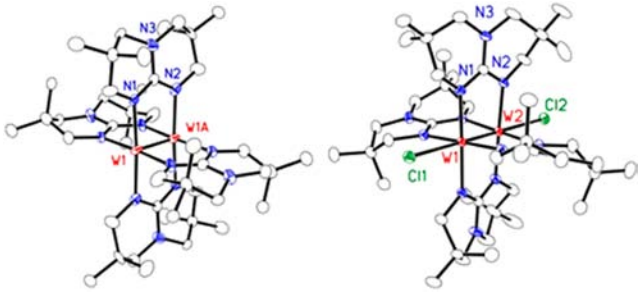

Figure 3. The structures of $1{\cdot}4CH_2Cl_2$ on the right and **3** on the left with displacement ellipsoids drawn at the 30% probability level. Solvent molecules in **1** and all hydrogen atoms have been removed for clarity.

guanidinate ligands spanning the ditungsten unit. For **1** and **2** the chlorine atoms occupy axial positions at distances of ∼2.85−2.98 Å (Table 4). The 2.98 Å distance is the longest of

Table 4. Comparison of Selected Bond Distances (Å) from Crystal Structures

	W−W	W−Cl	W−N
$W_2(hpp)_4Cl_2$[14]	2.250(2)	3.064(9)	2.08(1)
$W_2(TMhpp)_4Cl_2$	2.2483[2][a]	2.9781[4]	2.094[16]
$W_2(TEhpp)_4Cl_2$	2.2575(5)	2.8495[2]	2.104[9]
$W_2(hpp)_4$[14]	2.162(1)	–	2.128(5)
$W_2(TMhpp)_4$	2.1405(18)	–	2.147[4]

[a]Numbers in brackets are averages.

over 3500 W−Cl distances found in the CCDC and far beyond the mean of 2.42 Å, indicating only weak W−Cl bonding. The weakness of this bond is a contributing factor to the electrochemistry and the synthesis scheme shown in Scheme 1.

DISCUSSION

Photoelectron spectroscopy shows that these ditungsten tetraguanidinate molecules give up electrons at extremely low ionization energies around 3.4−3.5 eV, and yet these molecules are prepared by reduction with potassium, which holds its electron more tightly with an ionization energy of 4.34 eV. This presents a seeming conundrum. Taking the hpp complex as an example, why does the electron transfer from K to $W_2(hpp)_4^{1+}$ rather than the reverse direction from $W_2(hpp)_4$ to K^+? The answer lies largely in the geometric structure of the $W_2(hpp)_4$ molecule, which minimizes the solvent stabilization energy of its oxidized state compared to K^+. As a consequence of the greater stabilization of the K^+ positive ion in THF, the reduction potential of K/K^+ at −2.6 V is much more negative than the reduction potentials exhibited by these molecules in THF from −1.8 to −1.9 V, and thus the reduction of $W_2(hpp)_4^{1+}$ by K is thermodynamically favored.

A closer examination of the connection between the ionization energies and the reduction potentials leads to a better understanding of the strong reducing ability of these dimetal tetraguanidinate molecules in nonpolar organic solvents. Scheme 2 shows the connection starting from the

Scheme 2. Connection between the Observed Gas-Phase VIE (eV) and the Observed Solution Reduction Peak Potential (V, in THF), Both in Blue, with the DFT-Calculated Energy Contributions in Green

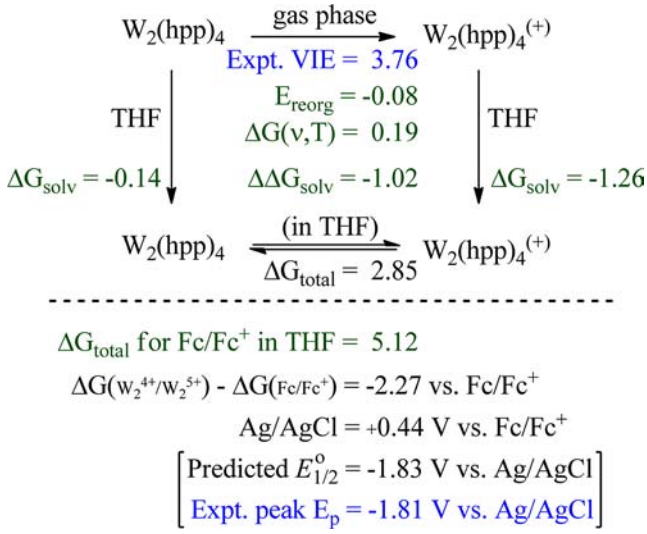

experimental gas-phase vertical ionization energy (VIE) of $W_2(hpp)_4$ shown in blue at the top and proceeds to the experimental $W_2^{5+/4+}$ potential measured in THF shown also in blue at the bottom. In contrast to the gas-phase spectroscopic energy (VIE) that is measured on a fast time scale, the solution potential measures an equilibrium (free energy) that involves the vibrational and thermal enthalpies and entropies of solvated species. These contributions are shown in green in the diagram as obtained from DFT computations (see Experimental Section), where E_{reorg} is the geometric reorganization energy of the positive ion from the structure of the neutral molecule, $\Delta G(\nu,T)$ includes the differences in zero-point vibrational energies and temperature-dependent H(T)-TS(T) contributions to the free energy at standard temperature and pressure, and ΔG_{solv} is the solvation stabilization energies of the neutral and cationic species.

The sum of these contributions gives the absolute free energy change for $W_2(hpp)_4/W_2(hpp)_4^+$ ($W_2^{4+/5+}$) in THF of 2.85 eV. A similar calculation for the ferrocene/ferrocene$^+$ couple (Fc/Fc^+) gives an absolute free energy change of 5.12 eV, so that

dx.doi.org/10.1021/ja408291k | J. Am. Chem. Soc. 2013, 135, 17889−17896

the ΔG for $W_2^{4+/5+}$ is 2.27 eV less than that of Fc/Fc^+. Since $\Delta G = -nFE$ and $F = 1$ for the conversion from eV to V, $E_{1/2}$ for $W_2^{4+/5+}$ in THF is projected to be −2.27 V vs Fc/Fc^+. In our experiments $E_{1/2}$ for the Fc/Fc^+ couple consistently occurred at +440 mV vs Ag/AgCl, so the calculated potential for $W_2(hpp)_4/W_2(hpp)_4^+$ vs Ag/AgCl is −1.83 V. This compares very closely to the observed peak position of −1.81 V measured in THF for $W_2(hpp)_4^{2+}(TFPB^-)_2$ ($TFPB^-$ is tetrakis[3,5-bis(trifluoromethyl)phenyl]borate).[10]

The primary point to recognize from Scheme 2 is that the solution reduction potential is determined primarily by two factors. First is the gas-phase vertical ionization energy, and second is the solvation stabilization of the positive ion. Because the overall structure of the molecule is largely determined by the structure of the bicyclic guanidinate ligands and their coordination to the metals, and the structure changes little from the neutral to the positive ion, the sum of the reorganization energy and vibrational/thermal contributions shifts the free energy by only about 0.2 eV. Errors in the modeling of these contributions are a small fraction of this number and have little effect on the full projected potential. The good agreement between the projected and the observed reduction potential then follows primarily from starting with an experimental gas-phase VIE and having a model that gives good account of the $\Delta\Delta G_{solv}$. Nearly all of the models tested were adequate in this regard for these molecules.

This is not to say that the DFT computations give a good account of the electron energies and bonding. All 75 functionals tested underestimated the VIE by an average of 0.6 eV (see SI, page S15). The optimized bond distances suggest that the computations underestimate the W−W bond strength, consistent with the low calculated VIE, and the computations consequently make the W−Cl bond slightly too strong. An underestimate of the VIE results directly in too negative a projected reduction potential. For example, an estimate of the $W_2^{5+/6+}$ potential according to Scheme 2 is forced to use a calculated VIE for the $W_2(hpp)_4^+$ cation because an experimental VIE of the cation is not possible by normal photoelectron techniques, and the projected potential is −1.60 V compared to the observed peak position of −0.97 V. The error is largely due to the underestimation of the VIE by the computations. This underscores the value of knowing the experimental ionization energies.

The ditungsten tetraguanidinate complexes in the electrochemical studies reported here have chlorine atoms coordinated to the tungsten atoms rather than $TFPB^-$ counterions. Nonetheless the reduction peaks in THF occur at very similar potentials to those of $W_2(hpp)_4^{2+}(TFPB^-)_2$. A question is the extent to which these dichloro complexes are soluted to ions in THF. As already mentioned the W−Cl interaction is weak as evidenced by the long distance, but the computations indicate that the W−Cl bond is only about one-third electrostatic. Scheme 3 shows the calculated equilibria for dissolution of $W_2(hpp)_4Cl_2$ into ions in THF, along with calculated reduction potentials for various species. The computations indicate that the neutral dichloro complexes are not appreciably soluted to ions in THF, but reduction increasingly favors dissociation of Cl^- from the complex. A driving force is the solvation energy of the Cl^- ion in THF (ΔG_{solv} literature 2.81 eV, DFT calcd 2.91 eV), which also shifts the reduction potential less negative. As mentioned above, the DFT calculations estimate the reduction potentials for these complexes too negative and may overestimate the W···Cl bond strength. But even with these

Scheme 3. DFT-Calculated Potentials and Equilibria for Reduction of $W_2(hpp)_4Cl_2$ in THF[a]

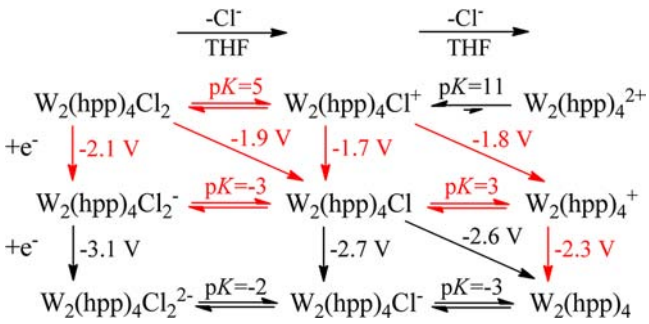

[a]The red lines show the low energy paths to formation of $W_2(hpp)_4$ + $2Cl^-$. Reduction promotes loss of chloride ions, replaced by THF molecules at the W_2 axial sites (not shown, see Figure 4 and the experimental section for the computational model).

overestimates Scheme 3 indicates that K in THF ($E_{1/2}$ literature −2.66 V, DFT calcd −2.64 V) will result in the reduction of $W_2(hpp)_4Cl_2$ to $W_2(hpp)_4$ + $2Cl^-$ in THF. The primary driving forces are the solvation stabilization of the Cl^- ions in comparison to the weak W···Cl interactions and the solvent stabilization of the K^+ ions in comparison to the weak stabilization of the $W_2(hpp)_4$ cations in THF.

The reason for the comparatively weak stabilization of the $W_2(hpp)_4^+$ cation in THF, in addition to the size of the molecule, is illustrated in Figure 4. The figure shows the

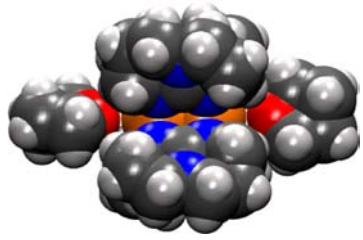

Figure 4. Optimized structure of $W_2(hpp)_4(THF)_2^+$ shown with van der Waals atomic radii. The van der Waals contacts impede close association of the THF solvent molecules with the W_2 core. Color codes: orange = tungsten; red = oxygen; blue = nitrogen; black = carbon; and gray = hydrogen atoms.

optimized structure of the $W_2(hpp)_4$ monocation with THF molecules in the axial sites. The van der Waals sizes of the hpp ligands impede the THF oxygen atoms from coming within van der Waals contact with the tungsten atoms and stabilizing the positive charge. In contrast the K^+ ion has the advantage of receiving the full stabilization from the THF solvent.

Because the complexes reported in this study have the advantage of being soluble in nonpolar organic solvents, it is interesting to compare the reducing power of these complexes in nonpolar solvents with the hypothetical case of K in a nonpolar solvent. Scheme 4 compares the favorable reduction directions in THF and hexane according to the free energies obtained from this computational model. The equilibrium switches direction from THF to hexane, such that in hexane $W_2(hpp)_4$ reduces K^+ to K. Also shown in Scheme 4 is the reducing power of $W_2(hpp)_4$ in comparison to decamethylcobaltocene—a commonly used strong reducing agent for stoichiometric reactions. $W_2(hpp)_4$ is a much stronger reducing agent than decamethylcobaltocene.

Scheme 4. DFT-calculated Free Energies of Reduction[a]

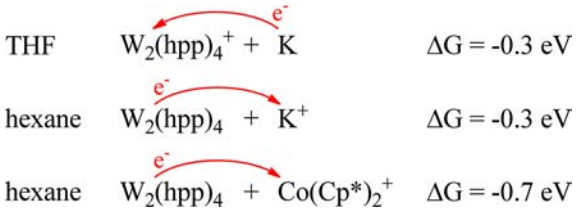

[a]Arrows show the thermodynamic direction of electron transfer. In THF potassium is a stronger reductant than $W_2(hpp)_4$, but in hexane the reverse is true. $W_2(hpp)_4$ is a stronger reductant than decamethylcobaltocene in all solvents.

CONCLUSIONS

Analogues of the most easily ionized molecule have been prepared in good yields. The ditungsten compounds with four bridging bicyclic guanidinate ligands have very low ionization energies and very negative oxidation potentials. Compounds **3** and **4** are thermally stable and very soluble and stable in nonhalogenated, nonprotonated solvents such as THF, toluene, benzene, and even hexanes. These properties make them ideal candidates for use as strong reducing agents.

Finally, it is worth noting how a field that began 50 years ago with the description of the quadruple bond in science[15] has moved from being an intellectual curiosity to the production of the strongest reducing agent in nonpolar solvents in a designed and systematic fashion. As noted, **3** and **4** owe their properties to a destabilization of the δ bond caused by the guanidinate groups.[16] Without a quadruple bond these compounds would not behave the way they do.

EXPERIMENTAL SECTION

Methods and Materials. All syntheses were carried out under N_2 using a Schlenk line equipped with a bubbler with a tube diameter of 2.54 cm and a column of ~5 cm of Hg. All manipulations preceding spectroscopic measurements were performed under Argon in a glovebox. Commercial solvents were treated as follows: acetonitrile was twice distilled under N_2, first from activated molecular sieves and then from CaH_2; THF was distilled from Na/K benzophenone; dichloromethane was dried and distilled from P_4O_{10}; toluene and isomeric hexanes were dried and degassed using a Glass Contour solvent purification system; *o*-dichlorobenzene was dried over freshly activated molecular sieves and degassed using vigorous bubbling of N_2 immediately before use. Tungsten hexacarbonyl, was purchased from commercial sources; HTMhpp and HTEhpp were prepared according to the literature procedures.[17]

Instrumentation and Characterization. ^{1}H NMR spectra were recorded on a Mercury 300 spectrometer with chemical shifts referenced to the protonated solvent residue. Mass spectrometry data (electrospray ionization, ESI) were recorded at the Laboratory for Biological Mass Spectrometry at Texas A&M University using an MDS Series Qstar Pulsar with a spray voltage of 5 kV. Elemental analyses were performed by Robertson Microlit Laboratories, Inc., Madison, NJ on crystalline samples that were previously washed with cold hexanes and dried overnight under vacuum. Infrared spectra were recorded in a Perkin-Elmer 16PC FT IR spectrophotometer using KBr pellets. Electronic spectra were recorded on a Shimadzu UV-2501 PC spectrophotometer. The differential pulse voltammograms were collected using a CH Instruments model-CHI620A electrochemical analyzer in a 0.1 M $Bu^n_4NPF_6$ solution in THF, using Pt working and auxiliary electrodes, a Ag/AgCl reference electrode, and a scan rate of 100 mV/s. All potential values are referenced to the Ag/AgCl electrode and under the present experimental conditions, the $E_{1/2}$ for the Fc^+/Fc couple consistently occurred at +440 mV.

Syntheses. *$W_2(TMhpp)_4Cl_2$, **1**.* A mixture of 0.240 g (0.682 mmol) of $W(CO)_6$ and 0.300 g (1.53 mmol) of HTMhpp was placed in an oven-dried 100 mL Schlenk flask equipped with a stir bar and filled with nitrogen. An aliquot of 15 mL of dried and oxygen-free *o*-dichlorobenzene was then added, and the flask was fitted with a previously oven-dried water-cooled coldfinger. The pale yellow reaction mixture was refluxed at 210 °C under nitrogen for 6−8 h.[18] During the reflux period, the color of the reaction mixture changed to deep yellow, orange, red, then to deep green. The solvent was removed by pumping under vacuum at 70 °C. The greenish-brown solid was extracted with 50 mL of toluene, and the mixture filtered under nitrogen using an oven-dried fritted-glass packed with Celite. The solvent from the green-brown solution was removed under vacuum, and the solid washed with hexanes (to remove a small amount of stopcock grease). The solid was dissolved in 10 mL of dichloromethane, and the solution was carefully layered with 40 mL of hexanes using a 60 mL Schlenk tube and a glass cap that was wrapped with Parafilm. After 4 weeks, dark green-brown, block-shaped crystals suitable for X-ray diffraction were obtained. Isolated yield 0.378 g, 91%.

Spectroscopic data for **1**: ^{1}H NMR: (C_6D_6, 300 MHz, 25 °C): δ_H = 4.17 ppm (s, 16H, $8CH_2$), 2.63 ppm (s, 16H, $8CH_2$), and 1.07 ppm (s, 48H, $16CH_3$). IR (KBr, cm^{-1}): ν = 2958, 1639, 1530, 1399, 1277, 1125, and 778. UV−vis: λ_{max} = 349.5 nm. ESI-MS: m/z = 1179.5, $[W_2(TMhpp)_4Cl]^+$; m/z = 572.25, $[W_2(TMhpp)_4]^{2+}$. Electrochemistry in THF vs Ag/AgCl: $E_{1/2}(1)_{THF}$ = −0.99 V, $E_{1/2}(2)_{THF}$ = −1.84 V. Elemental microanalysis calcd for $C_{44}H_{80}Cl_2N_{12}W_2$: C 43.46, H 6.63, N 13.82; found: C 43.40, H 6.88, N 13.64.

Crystallographic Data for **1**·$4CH_2Cl_2$. M_r = 1555.50, orthorhombic, *Pcca*, a = 24.256(5), b = 23.817(5), c = 25.791(5) Å, V = 14,900(5) Å^3, Z = 8, ρ_c = 1.387 Mg m^{-3}, T = 213(2) K, λ = 0.71073 Å. 92 163 reflections were collected, 16 921 independent [R(int) = 0.0371], which were used in all calculations. R_1 = 0.0270, wR_2 = 0.0609 for observed unique reflections [$F^2 > 2\sigma(F^2)$] and R_1 = 0.0631, wR_2 = 0.0677 for all unique reflections. Max. and min residual electron densities 1.573 and −2.422 eÅ^{-3}.

*$W_2(TEhpp)_4Cl_2$, **2**.* This compound was prepared similarly to **1** using a mixture of 0.240 g (0.682 mmol) of $W_2(CO)_6$ and 0.500 g (1.42 mmol) of HTEhpp in 15 mL of *o*-dichlorobenzene. After refluxing and removal of the solvent the green-brown solid was extracted with 50 mL of a mixture 4/1 hexanes/toluene, and then the mixture was filtered under nitrogen in an oven-dried fritted glass charged with Celite. After the solvent was removed under vacuum from the filtrate, the solid was covered overnight with hexanes at −20 °C, and then the supernatant liquid was removed using a cannula. The solid was dissolved in 20 mL of a 4:1 hexanes:toluene mixture. The tube was placed in a refrigerator at −30 °C. After 4 weeks dark green-brown, block-shaped crystals suitable for X-ray diffraction were collected. Isolated yield 0.443 g, 90%.

Spectroscopic Data for **2**. ^{1}H NMR: (C_6D_6, 300 MHz, 25 °C): δ_H = 4.10 pm (s, 16H, $8CH_2$), 2.81 ppm (s, 16H, $8CH_2$), 1.49 ppm (q, 32H, $16CH_2$) and 0.91 ppm. (s, 48H, $16CH_3$). IR (KBr, cm^{-1}): ν = 2961, 1637, 1534, 1380, 1275, 1123, and 807. UV−vis: λ_{max} = 347.5 nm. ESI-MS: m/z = 1403.7, $[W_2(TEhpp)_4Cl]^+$; m/z = 684.4, $[W_2(TEhpp)_4]^{2+}$. Electrochemistry in THF vs Ag/AgCl: $E_{1/2}(1)$ = −0.99 V, $E_{1/2}(2)$ = −1.90 V. Elemental microanalysis calcd for $C_{60}H_{112}Cl_2N_{12}W_2$: C 50.03, H 7.83, *N* = 11.67; found C 49.83, *H* = 7.69, N 11.46.

Crystallographic Data for **2**. M_r = 1440.22, monoclinic, $P2_1/c$, a = 16.894(4), b = 16.778(4), c = 22.935(6) Å, β = 97.635(5), V = 6443(3) Å^3, Z = 4, ρ_c = 1.485 Mg m^{-3}, T = 213(2) K, λ = 0.71073 Å. 42958 reflections collected, 14 770 independent [R(int) = 0.0729], which were used in all calculations. R_1 = 0.0518, wR_2 = 0.0968 for observed unique reflections [$F^2 > 2\sigma(F^2)$] and R_1 = 0.1018, wR_2 = 0.1077 for all unique reflections. Max. and min residual electron densities 2.353 and −1.423 eÅ^{-3}.

*$W_2(TMhpp)_4$, **3**.* A sample of 0.120 g (0.098 mmol) of dark green, solid $W_2(TMhpp)_4Cl_2$, that had been freshly washed with hexanes and then dried under vacuum was placed in a solid addition tube attached to a flask equipped with a stir bar and 0.30 g of freshly cut and cleaned

potassium metal in 15 mL of THF. An extremely dry glass frit joined with a side arm tube served as a cap to the reaction flask. After the solid was added to the flask, the mixture was degassed three times by the freeze−pump−thaw method and then heated using a gentle reflux (around 80−85 °C). After 30 min the dark green reaction mixture changed to brown and after 1 h to red-blood. After 2 h of reflux, the reaction mixture was cooled to room temperature, and half of the THF was removed under vacuum. The mixture was filtered through the attached fritted glass into a side-armed tube and brought to dryness under vacuum producing a deep-red, solid. Isolated yield 0.081 g, 72%. The solid was dissolved in 10 mL of toluene, set in a Schlenk tube under nitrogen with a glass cap protected with high vacuum grease and wrapped with Parafilm; the stopcocks and all joints were also wrapped with Parafilm and a septum was fitted to the side arm; the tube was placed in a freezer at −30 °C. After 2 weeks, very small dark-red, block-shaped crystals suitable for X-ray diffraction were collected. The product was stored in an ampule under argon.

Spectroscopic Data for **3**. ^{1}H NMR: (C_6D_6, 300 MHz, 25 °C): δ_H = 3.26 ppm (s, 16H, 8CH_2), 2.67 ppm (s, 16H, 8CH_2), and 1.15 ppm (s, 48H, 16CH_3). PES_{onset}: 3.74 ± 0.03 eV.

Crystallographic Data for **3**. M_r = 1144.90, triclinic, $P\bar{1}$, a = 10.197(6), b = 12.777(8), c = 13.452(8) Å, α = 112.441(9), β = 90.278(10), γ = 110.086(10)°, V = 1502.6(16) Å^3, Z = 1, ρ_c = 1.265 Mg m^{-3}, T = 213(2) K, λ = 0.71073 Å. 9272 reflections collected, 5169 independent [R(int) = 0.0871], which were used in all calculations. R_1 = 0.0862, wR_2 = 0.1562 for observed unique reflections [$F^2 > 2\sigma(F^2)$] and R_1 = 0.1541, wR_2 = 0.1744 for all unique reflections. Max. and min residual electron densities 5.483 and −2.426 eÅ^{-3}.

*W_2(TEhpp)$_4$, **4**.* This compound was prepared similarly to **3** using 0.14 g, 0.097 mmol of dark green solid W_2(TEhpp)$_4Cl_2$, 0.3 g of clean potassium metal and 15 mL of THF. After refluxing and filtration of the deep red reaction mixture, the solvent was removed to produce 0.095 g of a deep red solid. Isolated yield 0.095 g, 71%. The product was stored in a sealed ampule under argon.

Spectroscopic Data for **4**. ^{1}H NMR: (C_6D_6, 300 MHz, 25 °C): δ_H = 3.48 ppm (s, 16H, 8CH_2), 2.73 ppm (s, 16H, 8CH_2), 1.70 ppm (q, 16H, 8CH_2), 1.46 ppm (q, 16H, 8CH_2) and 0.92 ppm (s, 48H, 16CH_3). $PES_{vertical}$: 3.71 ± 0.03 eV.

PES. The gas-phase PES of W_2(TMhpp)$_4$ and W_2(TEhpp)$_4$ were recorded using an instrument that features a 36 cm radius, 8 cm gap hemispherical analyzer,[19] and custom-designed excitation source, sample cells, detection, and control electronics, and methods that have been described in detail previously.[20,21] The temperature was monitored using a "K"-type thermocouple passed through a vacuum feed through and attached directly to the sample cell. Samples of W_2(TMhpp)$_4$ and W_2(TEhpp)$_4$ were loaded into stainless steel cells and placed in the instrument using rigorous air-sensitive techniques. The data collection focused on determining the δ bond ionization energy. To avoid decomposition in the sample chamber of the cell, ampules containing the samples were broken off and placed directly in the ionization chamber.

The W_2(TMhpp)$_4$ sample began to sublime at 216 °C, and data were collected continually with gradually increasing temperature until 271 °C when the loaded sample was fully consumed. Complete spectra were collected every few minutes. The sample lasted for ∼2 1/2 h in the chamber without evidence of decomposition. The individual spectral scans showed the same ionization features, and the displayed spectra are the sum of the individual scans. Sublimation of the W_2(TEhpp)$_4$ sample began at around 317 °C and was still present at 340 °C. The signal was observed for about 1 h again without evidence of decomposition, and the displayed spectrum is the sum of the individual scans.

The $^2P_{3/2}$ peak of argon at 15.76 eV ionization energy is typically used for internal energy calibration, but over the course of the experiment sensitivity to the $^2P_{3/2}$ peak of Ar was lost. This often happens with molecules that are strong reductants, presumably because of the very large change in work function of the spectrometer when the sample condenses on the spectrometer surfaces. At this point the lamp was adjusted to emit He II photons in addition to He I photons. This allowed observation of the He self-ionization (by He II photons) at an apparent binding energy of 4.99 eV in the He I spectrum. This very sharp line is a convenient internal energy calibrant and is preferable for the calibration of low-energy ionizations. The resolution, as measured by the Ar peak before it was no longer visible, was ∼0.030 eV. The resolution for the W_2(TMhpp)$_4$ and W_2(TEhpp)$_4$ experiments, as measured by the He self-ionization, was 71 and 88 meV, respectively. Over the course of two separate data collections of W_2(TMhpp)$_4$, ∼800 counts of the full He I spectrum (Graphic S1) and an additional 400 counts of a close-up on the δ bond ionization were collected. For W_2(TEhpp)$_4$ ∼400 counts of the δ bond ionization were collected.

The ionization bands are represented analytically with asymmetric Gaussian peaks. As is typical for the first ionization bands of M_2(hpp)$_4$ molecules, a weak shoulder is observed on the high ionization energy side of the peak that necessitated the use of a second asymmetric Gaussian component to reasonably account for the total contour of the ionization intensity. The additional ionization intensity on the high ionization energy side of the first band is ascribed to the different puckered conformations that the hpp ligands can adopt in the molecules. The relative intensity of this component varies among the different M_2hpp$_4$ molecules. The broadening on the high ionization energy side of the W_2(TEhpp)$_4$ ionization is the greatest, where additional conformations due to the ethyl group orientations are possible. The vertical ionization energies are reported as the position of the main Gaussian peak in the analytical representation. The onset of ionization is the position at which the observed electron counts are significantly above a linear baseline through the peak.

Crystallographic data for 1−3. Crystals were coated with Paratone oil and mounted on a nylon Cryoloop affixed to a goniometer head. Data were collected at 213 K on a Bruker SMART 1000 CCD area detector system using omega scans of 0.3 deg/frame, with exposures of 60 (**1**), 50 (**2**), and 80 (**3**) seconds per frame, such that 1271 frames were collected for a full hemisphere of data. For each compound, the first 50 frames were collected again at the end of the data collection to monitor for crystal decay. No significant decomposition was observed. Cell parameters were determined using the program SMART.[22] Data reduction and integration were performed with the software package SAINT,[23] which corrects for Lorentz and polarization effects, while absorption corrections were applied by using the program SADABS.[24]

The structures were initially determined using the program XPREP from the SHELX software package.[25] Compound **1** was uniquely identified as belonging to the orthorhombic space group *Pcca* by its systematic absences. Because of residual disorder in solvent molecules, the Squeeze tool[26] from Platon[27] software was applied to finish the structure refinement. The structure contains two independent molecules in the asymmetric unit which means there are eight molecules per unit cell. Compound **2** gave a good refinement in the monoclinic space group $P2_1/c$. For this compound no interstitial solvent was found; there is one molecule in the asymmetric unit and four in the unit cell (Figure S4). Compound **3** was refined, following the Marsh's recommendation of choose the higher symmetry group,[28] in the triclinic space group $P\bar{1}$ instead of the noncentrosymmetric $P1$ that was the first choice suggested by the XPREP program; there is only one molecule in the asymmetric and unit cell. The methyl groups from the TMhpp ligands were disordered where the major components having occupancies between 50.3 and 54.2%. The structure contained interstitial disordered solvent that was treated using the Squeeze tool[26] from the Platon software.[27] Crystallographic data is provided in Tables S1−S5.

CCDC 760108, 7601109, and 760110 contain the supplementary crystallographic for **1−3**, respectively. These data can be obtained free of charge from The Cambridge Crystallographic Data Centre via www.ccdc.cam.ac.uk/data_request/cif/ .

Computational Model. Several density functional and basis set models were tested for their ability to account for the geometric structures and first gas-phase ionization energies of this class of ditungsten complexes. As pointed out in the discussion these features are the most important in relation to the reduction chemistry of these complexes. Functionals were tested at the level of the local density

approximation (LDA), the GGA with and without dispersion corrections, meta-GGA, hybrid, and meta-hybrid. Selected results with the Amsterdam Density Functional program[29] version adf2013.01 are shown in the SI. All functionals overestimated the W−W bond length by about 0.05 Å and underestimated the first ionization energy by as much as 0.6 eV. The LDA and GGA functionals had difficulty modeling the length of the weak W−Cl bonds, and the breaking of these bonds with reduction is important in the synthesis depicted in Scheme 1. Inclusion of dispersion with BJ damping[30] with the PBE[31] functional (PBE-D3) gave geometries that compared generally as well with the experimental W−Cl distance as the familiar meta-GGA and hybrid functionals and gave a somewhat better first ionization energy at much less computational cost, and therefore this model was selected for the remaining computations. The basis set selected for the geometry optimizations and electronic energies was double-ζ valence for hydrogen (DZ) and triple-ζ valence plus polarization (TZP, with nonvalence core) for all other atoms but tungsten. For tungsten an additional polarization function was added (TZ2P) to minimize basis set superposition errors (BSSE) for Cl^- dissociation with reduction, but as shown below BSSE is not a concern for this study because of the modeling approach. Relativistic effects are included by the zero order regular approximation[32] (ZORA). Solvation free energies are estimated by the conductor-like screening model[33] (COSMO) of solvation using default parameters.

Zero-point vibrational energies and thermal contributions to the free energy are computed at a lower level of theory because these terms have small contributions to the reduction chemistry for these complexes and to save computational costs. The functional was the Vosko−Wilk−Nusair[34] LDA with Stoll's[35] correction, and the basis set was TZP for tungsten and DZ for all other atoms. Harmonic vibrational frequencies were calculated analytically and used without scaling to calculate the gas-phase zero-point energies and thermal vibrational enthalpies and entropies. It is known that the gas-phase translational and rotational entropies overestimate the entropies in solution,[36] and this is especially a problem when the number of reactant molecules is different from the number of product molecules. We scaled the gas-phase translational and rotational entropies by 0.5 in solution similar to other adjustments in the literature.[36] We further mitigated this uncertainty by explicitly including solvent molecules to balance the number of reactant and product molecules. For example, for the release of the Cl^- ion with reduction, we explicitly occupied the vacated W_2 axial coordination site with a THF molecule as shown in Scheme 5 and pictured in Figure 4. This had the additional advantages

Scheme 5. Solvent Coordination to the Vacated Axial W_2 Coordination Site is Explicitly Included[a] in the Computational Model[b] in All Reaction Schemes

$$W_2(hpp)_4Cl_2 + THF \overset{+e^-}{\rightleftharpoons} W_2(hpp)_4Cl(THF) + Cl^-$$

[a]See Figure 4 for the structure of $W_2(hpp)_4(THF)_2$ for an example. [b]All four species are solvated according to the continuum model.

of (1) the basis set superposition error of a vacant site was eliminated, and (2) the explicit energy interaction of the THF molecule in the inner sphere in combination with the continuum solvation model for the outer sphere gave a better determination of the solvation energy. The success of this model was evidenced by the energies reported in Scheme 2.

■ ASSOCIATED CONTENT

Supporting Information

Crystallographic data and a cif file for **1**−**3**; wide scan PES of $W_2(TMhpp)_4$; ^1H NMR, IR, UV−vis, and ESI mass spectra; performance comparison of density functionals and basis sets; and a mol2 file of all computed molecule Cartesian coordinates that can be opened as text or viewed with a modeling program. This material is available free of charge via the Internet at http://pubs.acs.org.

■ AUTHOR INFORMATION

Corresponding Authors

murillo@tamu.edu

dlichten@email.arizona.edu

Present Addresses

[§] Department of Chemistry, Prairie View A&M University, Prairie View, TX, 77446.

[∥]Mission Heights Preparatory High School, 1376 E Cottonwood Ln., Casa Grande, AZ 85122

Author Contributions

[#]These authors contributed equally.

Notes

The authors declare no competing financial interest.

[▽]Deceased

■ ACKNOWLEDGMENTS

We thank the Robert A. Welch Foundation and Texas A&M University for financial support at TAMU. C.A.M also thanks the National Science Foundation for IR/D support. D.L.L. thanks The University of Arizona and the National Science Foundation (CHE-1111570).

■ REFERENCES

(1) For examples, see: (a) Chiarella, G. M.; Cotton, F. A.; Dalal, N. S.; Murillo, C. A.; Wang, Z.; Young, M. D. *Inorg. Chem.* **2012**, *51*, 5257−5263. (b) Chiarella, G. M.; Cotton, F. A.; Murillo, C. A. *Chem. Commun.* **2011**, *47*, 8940−8942. (c) Cotton, F. A.; Chiarella, G. M.; Dalal, N. S.; Murillo, C. A.; Wang, Z.; Young, M. D. *Inorg. Chem.* **2010**, *49*, 319−324. (d) Cotton, F. A.; Gu; Murillo, C. A.; Timmons, D. J. *J. Am. Chem. Soc.* **1998**, *120*, 13280−13281. (e) Cotton, F. A.; Huang, P.; Murillo, C. A.; Timmons, D. J. *Inorg. Chem. Commun.* **2002**, *5*, 501−504. (f) Cotton, F. A.; Daniels, L. M.; Murillo, C. A.; Timmons, D. J.; Wilkinson, C. C. *J. Am. Chem. Soc.* **2002**, *124*, 9249−9256. (g) Cotton, F. A.; Dalal, N. S.; Huang, P.; Ibragimov, S. A.; Murillo, C. A.; Piccoli, P. M. B.; Ramsey, C. M.; Schultz, A. J.; Wang, X.; Zhao, Q. *Inorg. Chem.* **2007**, *46*, 1718−1726.

(2) It is also relevant to note that guanidinate ligands characterized by a N−C(N)−N backbone have become increasingly important in coordination chemistry, and their anions have been used as ligands to stabilize a series of mononuclear as well as dinuclear species. See for example: (a) Foley, S. R.; Yap, G. P. A.; Richeson, D. S. *Polyhedron* **2002**, *21*, 619−627. (b) Soria, D. B.; Grundy, J.; Coles, M. P.; Hitchcock, P. B. *J. Organomet. Chem.* **2005**, *690*, 2278−2284. (c) Coles, M. P.; Hitchcock, P. B. *Organometallics* **2003**, *22*, 5201−5211. (d) Coles, M. P.; Hitchcock, P. B. *Dalton Trans.* **2001**, 1169−1171. (e) Coles, M. P.; Hitchcock, P. B. *Inorg. Chim. Acta* **2004**, *357*, 4330−4334. (f) Oakley, S. H.; Coles, M. P.; Hitchcock, P. B. *Inorg. Chem.* **2004**, *43*, 7564−7566. (g) Coles, M. P.; Hitchcock, P. B *Eur. J. Inorg. Chem.* **2004**, 2662−2672. (h) Irwin, M. D.; Abdou, H. E.; Mohamed, A. A.; Fackler, J. P., Jr. *Chem. Commun.* **2003**, 2882−2883. (i) Feil, F.; Harder, S. *Eur. J. Inorg. Chem.* **2005**, 4438−4443. (j) Wilder, C. B.; Reitfort, L. L.; Abboud, K. A.; McElwee-White, L. *Inorg. Chem.* **2006**, *45*, 263−268. (k) Rische, D.; Baunemann, A.; Winter, M.; Fischer, R. A. *Inorg. Chem.* **2006**, *45*, 269−277. (l) Duncan, A. P.; Mullins, S. M.; Arnold, J.; Bergman, R. G. *Organometallics* **2001**, *20*, 1808−1819. (m) Edelmann, F. T. *Chem. Soc. Rev.* **2009**, *38*, 2253−2268. (n) Chiarella, G. M.; Melgarejo, D. Y.; Rozanski, A.; Hempte, P.; Perez, L. M.; Reber, C.; Fackler, J. P., Jr. *Chem. Commun.* **2010**, *46*, 136−138. (o) Lee, R.; Yang, Y. Y.; Tan, G. K.; Tan, C.-H.; Wang, K.-W. *Dalton Trans.* **2010**, *39*, 723−725. (p) Ciabanu, O.; Fuchs, A.; Reinmuth, M.; Lebkücher, A.; Kaifer, E.; Wadepohl, H.; Himmel, H.-J. *Z. Anorg. Allg. Chem.* **2010**, *636*, 543−550. (q) Zheng, P.; Hong, J.;

Liu, R.; Zhang, Z.; Pang, Z.; Weng, L.; Zhou, X. *Organometallics* **2010**, *29*, 1284−1289. These and other analogous guanidine compounds have also been used in catalytic processes. For example, see: (a) Fu, X.; Tan, C.-H. *Chem. Commun.* **2011**, *47*, 8210−8222. (b) Wild, U.; Kaifer, E.; Himmel, H.-J. *Eur. J. Inorg. Chem.* **2011**, 4220−4233. (c) Li, L.; Liang, W. Y.; Han, K.-L.; He, G. Z.; Li, C. *J. Org. Chem.* **2003**, *68*, 8786−8789. (d) Deutsch, J.; Eckelt, R.; Köckritz, A.; Martin, A. *Tetrahedron* **2009**, *65*, 10365−10369. (e) Schulenberg, N.; Ciobanu, O.; Kaifer, E.; Wadepohl, H.; Himmel, H.-J. *Eur. J. Inorg. Chem.* **2010**, 5183−5188.

(3) Cotton, F. A.; Gruhn, N. E.; Gu, J.; Huang, P.; Lichtenberger, D. L.; Murillo, C. A.; Van Dorn, L. O.; Wilkinson, C. C. *Science* **2002**, *298*, 1971−1975.

(4) A'Court, R. Eur. Pat. App. 0198680, 1986.

(5) Hopfinger, A.; Söderlund, M.; Roni, S. *Finn. Pat.* 82445, 1990.

(6) Cotton, F. A.; Murillo, C. A.; Wang, X.; Wilkinson, C. C. *Dalton Trans.* **2007**, 3943−3951.

(7) Cotton, F. A.; Durivage, J. C.; Gruhn, N. E.; Lichtenberger, D. L.; Murillo, C. A.; Van Dorn, L. O.; Wilkinson, C. C. *J. Phys. Chem. B* **2006**, *110*, 19793−19798.

(8) Moore, C. E. Ionization Potentials and Ionization Limits Derived from the Analysis of Optical Spectra (NSRDS- NBS 34); National Bureau of Standards: Washington, DC, 1970.

(9) The peaks in the DPVs are a bit broad possibly because of the presence of various conformations of the ligands and/or dissociation of the Cl anions.

(10) Cotton, F. A.; Donahue, J. P.; Gruhn, N. E.; Lichtenberger, D. L.; Murillo, C. A.; Timmons, D. J.; Van Dorn, L. O.; Villagrán, D.; Wang, X. *Inorg. Chem.* **2006**, *45*, 201−213.

(11) Vannucci, A. K.; Snyder, R. A.; Gruhn, N. E.; Lichtenberger, D. L.; Enemark, J. H. *Inorg. Chem.* **2009**, *48*, 8856−8862.

(12) The yield is less than quantitative because of losses from solid clinging to the walls of the flask. It should also be noted that elemental analyses of **3** and **4** consistently showed lower experimental values for C and N by about 1% of the calculated values and therefore are not reported. This was presumably due to difficulties in handling of the extremely air-sensitive compounds.

(13) Ryan, M. F.; Richardson, D. E.; Lichtenberger, D. L.; Gruhn, N. E. *Organometallics* **1994**, *13*, 1190−1199 and references therein.

(14) Cotton, F. A.; Huang, P.; Murillo, C. A.; Wang, X. *Inorg. Chem. Commun.* **2003**, *6*, 121−126.

(15) Cotton, F. A.; Curtis, N. F.; Harris, C. B.; Johnson, B. F. G.; Lippard, S. J.; Mague, J. T.; Robinson, W. R.; Wood, J. S. *Science* **1964**, *145*, 1305.

(16) Because without a quadruple bond these compounds would not behave the way they do, we would like to dedicate this paper to the pioneers of the field of metal-to-metal multiple bonds, especially those in the previous reference: Cotton, Curtis, Harris, Johnson, Lippard, Mague, Robinson, and Wood, many of whom are still active in research.

(17) (a) Chiarella, G. M.; Cotton, F. A.; Ibragimov, S. A.; Murillo, C. A.; Wilkinson, C. C.; Young, M. D. *Polyhedron* **2013**, *58*, 7−12. (b) Cotton, F. A.; Durivage, J. C.; Gruhn, N. E.; Lichtenberger, D. L.; Murillo, C. A.; Van Dorn, L. O.; Wilkinson, C. C. *J. Chem. Phys. B* **2006**, *110*, 19793−19798 and references therein.

(18) To attain this temperature, the height of a mercury column in a bubbler must be about 5 cm. Alternatively, a Parr high-pressure reactor may be used.

(19) *Atomic, Molecular and Solid State Structure Studied by Means of Electron Spectroscopy*; Siegbahn, K., Nordling, C., Fahlman, A., Nordberg, R., Hamrin, K., Hedman, J., Johansson, G., Bergmark, T., Karlsson, S.-E., Lindgren, I., Lindberg, B., Eds; Almqvist and Wiksells: Uppsala, 1967; pp 1−274.

(20) Lichtenberger, D. L.; Kellogg, G.; Kristofzski, J. G.; Page, D.; Turner, S.; Klinger, G.; Lorenzen, J. *Rev. Sci. Instrum.* **1986**, *57*, 2366.

(21) Westcott, B. L.; Gruhn, N. E.; Enemark, J. H. *J. Am. Chem. Soc.* **1998**, *120*, 3382−3386 and references therein.

(22) *SMART for Windows NT*, version 5.618; Bruker Analytical X-ray Systems: Madison, WI, 2000.

(23) *SAINT for NT*, version 6.28A.; Bruker Analytical X-ray Systems: Madison, WI, 2001.

(24) *SADABS. Area Detector Absorption and other Corrections Software*, version 2.05; Bruker Advanced X-ray Solutions, Inc.: Madison, WI, 2001.

(25) Sheldrick, G. M. *SHELX-97 Programs for Crystal Structure Analysis*; Institüt für Anorganische Chemie der Universität Göttingen, Germany, 1998.

(26) van der Sluis, P.; Spek, A. L. *Acta Crystallogr.* **1990**, *A46*, 194−201.

(27) Spek, A. L. *PLATON, A Multipurpose Crystallographic Tool*; Utrecht University: Utrecht, The Netherlands, 2008.

(28) Marsh, R. E. *Acta Crystallogr.* **2009**, *B65*, 782−783.

(29) (a) te Velde, G.; Bickelhaupt, F. M.; van Gisbergen, S. J. A.; Fonseca Guerra, C.; Baerends, E. J.; Snijders, J. G.; Ziegler, T. *J. Comput. Chem.* **2001**, *22*, 931−967. (b) Fonseca Guerra, C.; Snijders, J. G.; te Velde, G.; Baerends, E. J. *Theor. Chem. Acc.* **1998**, *99*, 391−403. (c) *ADF2013*, SCM, Theoretical Chemistry; Vrije Universiteit: Amsterdam, The Netherlands; http://www.scm.com.

(30) Grimme, S.; Ehrlich, S.; Goerigk, L. *J. Comput. Chem.* **2011**, *32*, 1456−1465.

(31) Perdew, J. P.; Burke, K.; Ernzerhof, M. *Phys. Rev. Lett.* **1996**, *77*, 3865.

(32) van Lenthe, E.; Baerends, E. J.; Snijders, J. G. *J. Chem. Phys.* **1994**, *101*, 9783−9792.

(33) Klamt, A. *J. Phys. Chem.* **1995**, *99*, 2224−2235.

(34) Vosko, S. H.; Wilk, L.; Nusair, M. *Can. J. Phys.* **1980**, *58*, 1200−1211.

(35) Stoll, H.; Pavlidou, C. M. E.; Preuss, H. *Theor. Chim. Acta* **1978**, *49*, 143−149.

(36) Li, H.; Wen, M.; Wang, Z.-X. *Inorg. Chem.* **2012**, *51*, 5716−5727 and references therein.